Helical shell models for three-dimensional turbulence

R. Benzi,[1] L. Biferale,[1] R. M. Kerr,[2] and E. Trovatore[3]

[1]*Dipartimento di Fisica, Università di Tor Vergata, Via della Ricerca Scientifica 1, I-00133 Roma, Italy*
[2]*Geophysical Turbulence Program, National Center for Atmospheric Research, P.O. Box 3000, Boulder, Colorado 80307-3000*
[3]*INFM-Dipartimento di Fisica, Università di Cagliari, Via Ospedale 72, I-09124 Cagliari, Italy*
(Received 19 October 1995)

In this paper a class of shell models is studied, defined in terms of the interactions of two complex dynamical variables per shell, transporting positive and negative helicity, respectively. Following a decomposition into helical modes of the velocity Fourier components of Navier-Stokes equations [F. Waleffe, Phys. Fluids A **4**, 350 (1992)], classification of the helical interactions of the three modes in each triad leads to four different types of shell models. Free parameters are fixed by imposing the conservation of energy and of a "generalized helicity" H_α in the inviscid and unforced limit. For $\alpha = 1$ this nonpositive invariant looks exactly like helicity in the Fourier-helical decomposition of the Navier-Stokes equations. Long numerical integrations are performed, allowing the computation of the scaling exponents of the velocity increments and energy flux moments. The dependence of the models on the generalized helicity parameter α and on the scale parameter λ is also studied. Partial differential equations are finally derived in the limit when the ratio between shells goes to one.

PACS number(s): 47.27.Eq

I. INTRODUCTION

One of the most intriguing problems in three-dimensional (3D) turbulence is related to the understanding of the dynamical mechanism triggering and supporting the energy cascade from large to small scales. Following the Richardson scenario that energy should be transferred downward in scales, Kolmogorov [1] postulated that the energy cascade should follow a self-similar and homogeneous process entirely dependent on the energy transfer rate. This idea, plus the assumption of local isotropy and universality of the small scales, eventually led to a precise prediction on the statistical properties of the increments of turbulent velocity fields, that is, $\delta v(l) \sim |v(x+l) - v(x)|$, where at distances l depends solely on the dissipation or energy transfer $\epsilon(l)$ over scales l in the manner predicted by Kolmogorov [1] $\delta v(l) \sim [l\epsilon(l)]^{1/3}$. From this the scaling of moments of $\delta v(l)$, the structure functions, can be determined in terms of the statistics of $\epsilon(l)$,

$$S_p(l) \equiv \langle [\delta v(l)]^p \rangle = C_p \langle [\epsilon(l)]^{p/3} \rangle l^{p/3}, \qquad (1)$$

where C_p are constants and the scale l is supposed to be in the inertial range, i.e., much smaller than the integral scale and much larger than the viscous dissipation cutoff. If $S_p(l) \sim l^{\zeta(p)}$ and $\langle \epsilon^p(l) \rangle \sim l^{\tau(p)}$, then

$$\zeta(p) = p/3 + \tau(p/3). \qquad (2)$$

In [1] the $\epsilon(l)$ statistic is assumed to be l independent, or $\tau(p) = 0$, implying $\zeta(p) = p/3 \; \forall p$, in particular $\zeta(2) = \frac{2}{3}$ or the energy spectrum going as $k^{-5/3}$. While from a qualitative point of view Kolmogorov's intuition was a true breakthrough in the understanding of turbulence, his theory lacks quantitative agreement with experimental measurements of intermittency in physical space. In particular there are nontrivial scaling corrections to the "p over 3" Kolmogorov

prediction for the $\zeta(p)$ exponents. There are many experimental and numerical [2–7] results telling us that energy is transferred intermittently.

In order to understand energy transfer dynamics and related intermittent effects, besides analytical and direct numerical approaches, two other possible choices are building simple random processes for the chaotic energy transfer among different scales [8–11] or studying a dynamical deterministic model. This paper will be devoted to the study of a different class of shell models: deterministic dynamical models, which in the past 20 years have been particularly successful. Shell models concentrate all the dynamical interactions into a few degrees of freedom at different scales, retaining the nonlinear structure of Navier-Stokes (NS) equations but neglecting completely their spatial location and losing most of their three-dimensional vector properties. A one-dimensional chain of interacting Fourier modes is constructed with simplifications so strong that only *a posteriori* can one say whether or not the model is interesting and reliable.

The most popular shell model, the Gledzer-Ohkitani-Yamada (GOY) model [12–18], has been shown to predict scaling properties for $\zeta(p)$ (for a suitable choice of the free parameters) similar to what is found experimentally. Recently, it was pointed out that the GOY model conserves in the inviscid, unforced limit two quadratic quantities. The first quantity is *energy*, while the second is, roughly speaking, the equivalent of *helicity* in 3D turbulence [17]. It has been suggested that both the GOY helicity [18] and the helicity in the NS equations [19,20] play roles in triggering the intermittent nature of the energy cascade.

Until recently, shell models have been derived strictly from basic phenomenological considerations about turbulence and required very strong assumptions about why the cascade would follow the particular path proposed. From the recent emphasis on the role played by the helicity and other

conserved quantities in shell models [21,18], a different class of shell models, based upon a helical decomposition of interactions between modes in the Navier-Stokes equations [22] and less on pure phenomenology, has been suggested [18]. In this way it is possible to obtain a second nonpositive defined invariant closer to the definition of helicity in the Navier-Stokes equations. The models, which have two complex variables per shell, are generalizations of the GOY model with helical structures that include all the possible helical interactions in the Navier-Stokes equations. In fact, two of the models can be reduced to variations of the GOY model. The derivation of the general class of these shell models and a study of their statistical properties will be the focus of this paper.

Our immediate aim consists in trying to understand the importance of the transfer of both energy and helicity in Navier-Stokes equations by examining the nontrivial dynamics shown by this different class of helical-shell models. Eventually, we want to take what is uncovered by the different shell models and use these properties to suggest alternate direct simulations aimed at understanding the turbulence cascade. When the stage of relating shell models to direct simulations is reached, questions about the compatibility of the properties of shell models with our understanding of the properties of the turbulent cascade coming from statistical studies of turbulence will arise. In anticipation of this step, some of these points will be addressed in the Conclusion.

The outline of the paper is as follows. In Sec. II the GOY model is reviewed. In Sec. III the different class of helical-shell models is introduced. In Sec. IV the basic triad interactions within three contiguous shells are studied. Section V contains the results of our numerical simulations. In Sec. VI partial differential equations (PDEs) for the continuum limit (ratio between shells that goes to one) are derived. Conclusions follow in Sec. VII.

II. THE GOY MODEL

The GOY model can be seen as a severe truncation of the Navier-Stokes equations. It retains only one complex mode u_n as a representative of all Fourier modes in the shell of wave numbers k between $k_n = k_0 \lambda^n$ and k_{n+1}, λ being an arbitrary scale parameter ($\lambda > 1$), usually taken to be equal to 2. The dynamics is governed by the following set of complex coupled ordinary differential equations, where only couplings with the nearest and next nearest shells are kept:

$$\frac{d}{dt} u_n = i k_n (a u^*_{n+1} u^*_{n+2} + b u^*_{n+1} u^*_{n-1} + c u^*_{n-1} u^*_{n-2}) - \nu k_n^2 u_n$$

$$+ \delta_{n,n_0} f, \qquad (3)$$

where ν is the viscosity, f is the external forcing acting on a large scale n_0, and a,b,c are three free parameters. By adjusting the time scale we can always fix $a=1$; the possible choices for b,c are restricted by imposing the conservation of two quadratic quantities in the inviscid and unforced limit

$$W_{1,2} = \sum_n z_{1,2}^n |u_n|^2, \qquad (4)$$

where $z_{1,2}$ are the solutions of the quadratic equation

$$c\lambda^2 z^2 + b\lambda z + a = 0. \qquad (5)$$

In order to stay as close as possible to the NS equations, we require that one of the two conserved quantities is the energy, i.e., $z_1 = 1$,

$$W_1 = E = \sum_n |u_n|^2. \qquad (6)$$

If we rewrite

$$\lambda b = -\epsilon, \quad \lambda^2 c = \epsilon - 1, \qquad (7)$$

we are left with only two (λ and ϵ) of the original four free parameters. The second quadratic invariant is

$$W_2 = H = \sum_n (\epsilon - 1)^{-n} |u_n|^2. \qquad (8)$$

The characteristics of this second invariant change by changing ϵ: when $\epsilon < 1$ it is not positive definite (as helicity in three dimensions), while if $\epsilon > 1$ it is positive definite (as enstrophy in two dimensions). Expression (8) can be rewritten as

$$H_\alpha = \sum_n \chi(\epsilon)^n k_n^{\alpha(\epsilon,\lambda)} |u_n|^2, \qquad (9)$$

where $\chi(\epsilon) = \text{sgn}(\epsilon - 1)$ and the parameter α is related to ϵ and λ by

$$|\epsilon - 1| = \lambda^{-\alpha}. \qquad (10)$$

Our interest here is to consider how well the dynamics of a 3D turbulent flow is reproduced by the model: Only ϵ in the range $0 < \epsilon < 1$ will be taken, in order to have a nonpositive definite second invariant. Indeed, for $\alpha = 1$ our "generalized helicity" $H_\alpha = \Sigma_n (-1)^n k_n^\alpha |u_n|^2$ has physical dimensions coinciding with the 3D Navier-Stokes helicity. The two free parameters of the model can be taken to be λ (the ratio between adjacent shells) and α. The two coefficients b and c can be rewritten as

$$b = \lambda^{-\alpha-1} - \lambda^{-1}, \quad c = -\lambda^{-\alpha-2}. \qquad (11)$$

Such a class of models has a highly nontrivial dynamical behavior. Intermittency of the energy transfer and multifractal nature of energy dissipation have been studied in [12–16].

It turns out that the values of the $\zeta(p)$'s are not universal, depending on the choice of ϵ and λ [15,17]. Nevertheless, Kadanoff et al. [17] verified that the scaling exponents are invariant along the curve in the (ϵ,λ) plane where both energy and helicity are conserved, i.e., the curve at $\alpha(\epsilon,\lambda) = 1$. This suggested that the second invariant plays a crucial role in the model dynamics. More recently, Biferale and Kerr [18] attributed to the helicity the role of triggering the intermittent cascade of the energy from large to small scales. These considerations, together with the observation that this "GOY helicity" is only partially consistent with the NS helicity (i.e., it presents an asymmetry between odd and even shells that does not have any counterpart in physical flows), persuaded us to study a modified shell model [18],

with two complex variables in each shell, carrying helicity of opposite sign, in order to obtain a second invariant closer to the NS helicity. In the following section we introduce this class of shell models, whose nonlinear interactions are constructed on the basis of a helical decomposition of the NS equations in the Fourier space.

III. HELICAL-SHELL MODELS

In order to introduce two helical variables per shell we refer to the velocity field in NS equations, expanded in a Fourier series [22]. The velocity vector can be represented in terms of its projection on an orthogonal basis formed by $\mathbf{k}$, $\mathbf{h}_+$, and $\mathbf{h}_-$. The two basis vectors $\mathbf{h}_+$ and $\mathbf{h}_-$ can be chosen to be the eigenmodes of the curl operator

$$i\mathbf{k}\times\mathbf{h}_s = sk\mathbf{h}_s, \tag{12}$$

where $s=\pm 1$. This corresponds to an expansion of the velocity vector into helical modes

$$\mathbf{u}(\mathbf{x}) = \sum_{\mathbf{k}} \mathbf{u}(\mathbf{k})\exp(i\mathbf{k}\cdot\mathbf{x})$$

$$= \sum_{\mathbf{k}} [u^+(\mathbf{k})\mathbf{h}_+ + u^-(\mathbf{k})\mathbf{h}_-]\exp(i\mathbf{k}\cdot\mathbf{x}). \tag{13}$$

The real flow velocity corresponding to the plus (minus) mode rotates clockwise (counterclockwise) as one moves in the direction of $\mathbf{k}$, thereby forming a left-handed (right-handed) helix; the vorticity vector of such a flow is parallel (antiparallel) to the velocity and the helicity is maximum (minimum). The kinetic energy and helicity are given by:

$$E = \sum_{\mathbf{k}} E(\mathbf{k})$$

$$= \sum_{\mathbf{k}} \tfrac{1}{2} \mathbf{u}(\mathbf{k})\cdot\mathbf{u}^*(\mathbf{k})$$

$$= \sum_{\mathbf{k}} [|\mathbf{u}^+(\mathbf{k})|^2 + |\mathbf{u}^-(\mathbf{k})|^2], \tag{14}$$

$$H = \sum_{\mathbf{k}} H(\mathbf{k})$$

$$= \sum_{\mathbf{k}} \tfrac{1}{2} \mathbf{u}(\mathbf{k})\cdot\omega^*(\mathbf{k})$$

$$= \sum_{\mathbf{k}} k[|\mathbf{u}^+(\mathbf{k})|^2 - |\mathbf{u}^-(\mathbf{k})|^2].$$

Plugging Eq. (13) into the NS equations yields the dynamical evolution for the complex amplitudes $u^{s_k}(\mathbf{k},t)$ $(s_k=\pm 1)$ [22]:

$$\frac{d}{dt}u^{s_k}(\mathbf{k}) + \nu k^2 u^{s_k}(\mathbf{k}) = \sum_{\mathbf{k}+\mathbf{p}+\mathbf{q}=0} \sum_{s_p,s_q} g_{\mathbf{k},\mathbf{p},\mathbf{q}}(s_p p - s_q q)$$

$$\times [u^{s_p}(\mathbf{p})u^{s_q}(\mathbf{q})]^*. \tag{15}$$

The geometric factor $g_{\mathbf{k},\mathbf{p},\mathbf{q}} = -\tfrac{1}{4}(\mathbf{h}_{s_\mathbf{k}}\times\mathbf{h}_{s_\mathbf{p}}\cdot\mathbf{h}_{s_\mathbf{q}})^*$ can be developed and factorized

$$g = r\frac{s_k k + s_p p + s_q q}{p}, \tag{16}$$

where r is a function of the triad shape only [22].

Eight different types of interaction between three modes $u^{s_k}(\mathbf{k})$, $u^{s_p}(\mathbf{p})$, and $u^{s_q}(\mathbf{q})$ with $|\mathbf{k}|<|\mathbf{p}|<|\mathbf{q}|$ are allowed according to the value of the triplet $(s_k,s_p,s_q) = (\pm 1,\pm 1,\pm 1)$: Among them, only four are independent, the coefficients of the interaction with reversed helicities $(-s_k,-s_p,-s_q)$ being identical to those with (s_k,s_p,s_q) [22]:

$$(s_k,s_p,s_q) = (+,-,+) \text{ or } (-,+,-),$$

$$(s_k,s_p,s_q) = (+,-,-) \text{ or } (-,+,+),$$

$$(s_k,s_p,s_q) = (+,+,-) \text{ or } (-,-,+),$$

$$(s_k,s_p,s_q) = (+,+,+) \text{ or } (-,-,-).$$

(corresponding to models 1–4, respectively). The equations corresponding to the single interaction (s_k,s_p,s_q) have the form (omitting viscosity and forcing)

$$\dot{u}^{s_k} = r(s_p p - s_q q)\frac{s_k k + s_p p + s_q q}{p}(u^{s_p}u^{s_q})^*,$$

$$\dot{u}^{s_p} = r(s_q q - s_k k)\frac{s_k k + s_p p + s_q q}{p}(u^{s_q}u^{s_k})^*, \tag{17}$$

$$\dot{u}^{s_q} = r(s_k k - s_p p)\frac{s_k k + s_p p + s_q q}{p}(u^{s_k}u^{s_p})^*.$$

Each interaction independently conserves both energy and helicity on a single triad. The dynamical system (17) composed by a single triad can be considered as the basic brick of the semi-infinite chain leading to the transfer of energy in turbulent flow. By studying its stability properties it is possible to understand how energy and helicity are transferred among different wave vectors belonging to the same triad.

Following [22], we distinguish two different kinds of dynamics: For the cases corresponding to the choices 1 and 3 of the triad helicities, the unstable wave vector is the smallest one, while for cases 2 and 4 the unstable wave vector is the medium one. This very simple analysis suggests that by linking together a series of triads we should have a forward energy transfer for cases 1 and 3 and both forward and backward (competing) energy transfers for cases 2 and 4.

In a turbulent flow the direction of energy transfer is dynamically controlled by the triple correlation $\langle u^{s_k}(\mathbf{k})u^{s_p}(\mathbf{p})u^{s_q}(\mathbf{q})\rangle$. It is reasonable to argue that the statistical properties of $\langle u^{s_k}(\mathbf{k})u^{s_p}(\mathbf{p})u^{s_q}(\mathbf{q})\rangle$ are such that the overall direction in energy transfer coincides with the simplified behavior inferred from the stability study of the single triad (*instability assumption* in [22]). For instance, it is easy to estimate, by using the instability assumption, what would be the net energy transfer in the above four cases if the energy spectrum had the Kolmogorov scaling $E(k)=k^{-5/3}$

TABLE I. Helicity indices of Eqs. (18) for the four models.

Model	s_1	s_2	s_3	s_4	s_5	s_6
1	+	−	−	−	−	+
2	−	−	+	−	+	−
3	−	+	−	+	−	−
4	+	+	+	+	+	+

TABLE II. Coefficients of Eqs. (18) for the four models.

Model	b	c
1	$\dfrac{\lambda^{-\alpha}-\lambda^{\alpha}}{\lambda^{\alpha+1}+\lambda}$	$\dfrac{-\lambda^{-1}-\lambda^{-\alpha-1}}{\lambda^{\alpha+1}+\lambda}$
2	$\dfrac{\lambda^{-\alpha}+\lambda^{\alpha}}{-\lambda^{\alpha+1}+\lambda}$	$\dfrac{-\lambda^{-1}-\lambda^{-\alpha-1}}{-\lambda^{\alpha+1}+\lambda}$
3	$\dfrac{-\lambda^{-\alpha}-\lambda^{\alpha}}{\lambda^{\alpha+1}+\lambda}$	$\dfrac{-\lambda^{-1}+\lambda^{-\alpha-1}}{\lambda^{\alpha+1}+\lambda}$
4	$\dfrac{\lambda^{-\alpha}-\lambda^{\alpha}}{\lambda^{\alpha+1}-\lambda}$	$\dfrac{+\lambda^{-1}-\lambda^{-\alpha-1}}{\lambda^{\alpha+1}-\lambda}$

[22]: 1 and 3, direct energy cascade from large to small scales; 4, reverse energy cascade from small to large scales; and 2, direct (reverse) energy cascade for local (nonlocal) triads.

The helical decomposition of the NS equations suggested to us the opportunity of defining a different GOY-like shell model for each one of the above four classes. In each shell we will have two complex dynamical variables u_n^+ and u_n^-, transporting positive and negative helicity, respectively,

$$\dot{u}_n^+ = ik_n(a_j u_{n+2}^{s_1} u_{n+1}^{s_2} + b_j u_{n+1}^{s_3} u_{n-1}^{s_4} + c_j u_{n-1}^{s_5} u_{n-2}^{s_6})^*$$
$$- \nu k_n^2 u_n^+ + \delta_{n,n_0} f^+,$$

$$\dot{u}_n^- = ik_n(a_j u_{n+2}^{-s_1} u_{n+1}^{-s_2} + b_j u_{n+1}^{-s_3} u_{n-1}^{-s_4} + c_j u_{n-1}^{-s_5} u_{n-2}^{-s_5})^*$$
$$- \nu k_n^2 u_n^- + \delta_{n,n_0} f^-, \qquad (18)$$

where $j = 1, \ldots, 4$ labels the four different models and the helicity indices in the nonlinear interactions are easily found for each of the four cases (see Table I).

The coefficients a_j, b_j, c_j are determined by imposing, as usual, the energy conservation

$$\frac{d}{dt}E = \frac{d}{dt}\left(\sum_n (|u_n^+|^2 + |u_n^-|^2)\right) = 0, \qquad (19)$$

which leads to the same relation for all models:

$$a_j + b_j\lambda + c_j\lambda^2 = 0. \qquad (20)$$

By imposing also the conservation of the generalized helicity

$$\frac{d}{dt}H_\alpha = \frac{d}{dt}\sum_n k_n^\alpha(|u_n^+|^2 - |u_n^-|^2) = 0 \qquad (21)$$

we obtain different relations for the four models, respectively,

$$a_1 - \lambda^{\alpha+1}b_1 + \lambda^{2(\alpha+1)}c_1 = 0,$$

$$a_2 - \lambda^{\alpha+1}b_2 - \lambda^{2(\alpha+1)}c_2 = 0,$$

$$a_3 + \lambda^{\alpha+1}b_3 - \lambda^{2(\alpha+1)}c_3 = 0,$$

$$a_4 + \lambda^{\alpha+1}b_4 + \lambda^{2(\alpha+1)}c_4 = 0.$$

Fixing $a_j = 1$, one then finds the expressions for the coefficients b_j and c_j in terms of the parameters λ and α (see Table II).

Let us remark two important facts. First, model 1 is nothing but two masked and uncorrelated versions of the original GOY model, with dynamical variables $(u_1^+, u_2^-, u_3^+, \ldots)$ and $(u_1^-, u_2^+, u_3^-, \ldots)$ respectively; rewriting the coeffi-

cients b_1 and c_1 in terms of the usual parameters λ and ϵ, one can easily recover the standard GOY model coefficients. Second, model 4 is also formed by two independent sets of variables $(u_1^+, u_2^+, u_3^+, \ldots)$ and $(u_1^-, u_2^-, u_3^-, \ldots)$, each of them conserving separately a positive-definite quantity similar to enstrophy in two dimensions. Thus model 4 is equivalent to two uncorrelated GOY models for 2D turbulence [23,24].

The fact that the model 1 is formed by two uncorrelated GOY models is clearly due to our choice of taking only first and second neighbor interactions. Model 4, on the other hand, will always be the sum of two separated models for any choice of the interacting modes composing the triads.

In the following, we will refer to the properties of model 1, intending the corresponding properties of the GOY model. Model 4 will be studied only for completeness.

IV. ONE-TRIAD SYSTEMS

Following the *instability assumption* [22] that connects the single-triad dynamics with the global statistical behavior of a multitriads flow, we repeat the analog stability study for the three-shell, single-triad system. By isolating three shells of wave numbers k_1, k_2, k_3, we can inspect their dynamical properties as determined by their mutual interactions. For the positive-helicity modes we have

$$\dot{u}_1^+ = ik_1(u_3^{s_1} u_2^{s_2})^*,$$

$$\dot{u}_2^+ = ik_2 b_j(u_3^{s_3} u_1^{s_4})^*, \qquad (22)$$

$$\dot{u}_3^+ = ik_3 c_j(u_2^{s_5} u_1^{s_6})^*,$$

where $j = 1, \ldots, 4$ for the four models. An analogous set of equations holds for the negative-helicity modes, changing the sign of the helicity index of all variables. This system conserves both energy and helicity. The corresponding equations for the energies are

$$\dot{E}_1 = A,$$

$$\dot{E}_2 = b_j\lambda A, \qquad (23)$$

$$\dot{E}_3 = c_j\lambda^2 A,$$
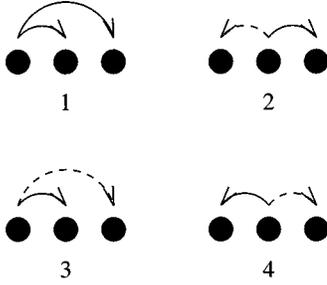
FIG. 1. Energy exchange in the one-triad system for the four models. Dashed (solid) arrows point towards the mode that receives less (more) energy.

where $A = 2k_1 \text{Im}[(u_3^{s_1} u_2^{s_2} u_1^{+}) + (u_3^{-s_1} u_2^{-s_2} u_1^{-})]$.

As found in [22], we know that the unstable mode is the smallest mode for interactions 1 and 3 and the medium mode for interactions 2 and 4. In order to have a deeper understanding of the energy transfer dynamics, we have performed several integrations of Eqs. (22), using the parameter values $\lambda = 2$, $\alpha = 1$, and $k_1 = 2^{-4}$ and different initial conditions. This analysis, performed on all four models, gives the following results: For model 1, mode 1 gives energy equally to modes 2 and 3; for model 2, mode 2 gives more energy to mode 3 than to mode 1; for model 3, mode 1 gives more energy to mode 2 than to mode 3; and for model 4; mode 2 gives more energy to mode 1 than to mode 3. These energy exchanges are summarized in Fig. 1.

Behaviors 1 and 4 have already been noticed by Ditlevsen and Mogensen [25] for the 3D and the 2D GOY model, respectively. It is also interesting to investigate how these properties are modified when varying the α parameter in the models. Considering that in Eq. (23) the sum of the three right-hand sides must be zero and normalizing to one the energy rate on the unstable shell, one can evaluate how the energy sharing between the other shells is affected by changing α (see Fig. 2).

In model 1 there is a clear dependence on α. As this parameter increases, more and more energy is captured by mode 2. For $\alpha > 1$, the energy gained by mode 2 become greater than the energy gained by mode 3, leading to a more local energy transfer.

Model 3 is remarkably independent of α, as we shall see in the following. This fact has very important consequences for the intermittent dynamics of the complete shell model.

Model 2 has a trend analogous to that of model 1, but with more drastic consequences: At $\alpha \sim 1.27$ the mode that receives most of the energy from the unstable mode is 1 instead of 3. This would suggest a change in the direction of the flux from downward to upward.

In model 4 the mode that receives most of the energy remains mode 1, for all values of α, with a consequent reverse energy flux in all cases (as it must be, since model 4 is a couple of 2D GOY models).

What emerges from this analysis is that the behavior of the models seems to depend on the choice of the free parameter α, sometimes with strong consequences (such as the change in direction of the flux in model 2). The only remarkable exception is the very low dependence of model 3.

Concerning helicity, we can consider the equations

$$\dot{H}_1(\alpha) = B,$$

$$\dot{H}_2(\alpha) = \eta_2 b_j \lambda^{\alpha+1} B, \qquad (24)$$

$$\dot{H}_3(\alpha) = \eta_3 c_j \lambda^{2(\alpha+1)} B,$$

where $B = 2k_1^{\alpha+1} \text{Im}[(u_3^{s_1} u_2^{s_2} u_1^{+}) - (u_3^{-s_1} u_2^{-s_2} u_1^{-})]$ and η_2 and η_3 depend on the particular model considered (see Table III). By performing the same analysis done for the energy evolution, one can conclude that helicity is transferred in different ways, as depicted in Fig. 3.

Since helicity is a nonpositive definite quantity, forward (backward) transfer of positive (negative) helicity is equivalent to backward (forward) transfer of negative (positive) he-
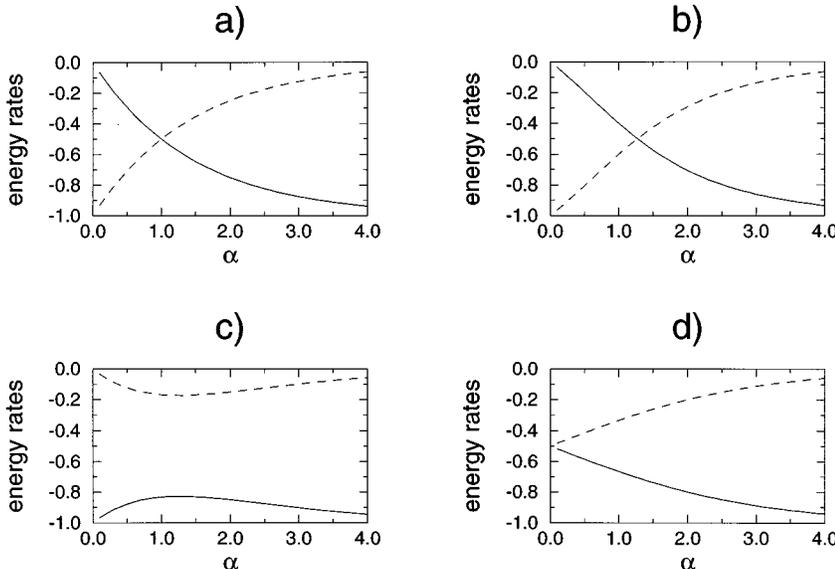
FIG. 2. Variations with α of the energy rates in the one-triad system for the four models. For each model $\dot{E}$ is shown for the two modes that receive energy from the unstable mode, whose energy rate is always kept equal to 1. (a) $\dot{E}_2$ (solid line) and $\dot{E}_3$ (dashed line) vs α for model 1 ($\dot{E}_1 = 1$); (b) $\dot{E}_1$ (solid line) and $\dot{E}_3$ (dashed line) vs α for model 2 ($\dot{E}_2 = 1$); (c) $\dot{E}_2$ (solid line) and $\dot{E}_3$ (dashed line) vs α for model 3 ($\dot{E}_1 = 1$); (d) $\dot{E}_1$ (solid line) and $\dot{E}_3$ (dashed line) vs α for model 4 ($\dot{E}_2 = 1$).

TABLE III. Factors in Eqs. (24) for the four models.

Model	η_2	η_3
1	-1	$+1$
2	-1	-1
3	$+1$	-1
4	$+1$	$+1$

licity. In view of this trivial remark, arrows in Fig. 3 have only a visual value, indicating how helicity (with its own sign) is redistributed among shells.

Let us note that models 1 and 3 show a very different pattern in the helicity exchange among shells. This can be the explanation of the very different scaling properties shown by the two models when varying α (see Sec. V). For example, we could argue that the dramatic dependence of the energy exchange on the α parameter in models 1 and 2, together with the well defined direction of the helicity transfer, can somehow enhance the role played by the second invariant with respect to the other two models. In the next section we will check these arguments by performing a numerical study of Eq. (18).

V. NUMERICAL ANALYSIS (MODEL 3)

In this section we will concentrate on the study of the statistical properties of model 3 compared with the already known results for the GOY model (model 1). Model 3, different from model 2, shows for any value of α a forward energy transfer. We integrated Eqs. (18) for model 3 using the standard parameters $\alpha=1$, $\lambda=2$, $k_0=2^{-4}$, $f^\pm =5(1+i)\times10^{-3}$, $n_0=1$, and $\nu=10^{-7}$ and a total number of shells equal to $N=22$ and 26. In the numerical integration we used a fourth-order Runge-Kutta method, with a time step varying between $dt=10^{-5}$ (for the simulations with 22 shells) and 10^{-6} (for the cases with 26 shells). Most of the results presented here are for the case $N=22$, with a number of iterations of the order of hundred of millions, which corresponds roughly to several thousands of eddy turnover times at the integral scale. Stationarity is checked by monitoring the total energy evolution.

The quantities we have looked at are the structure functions
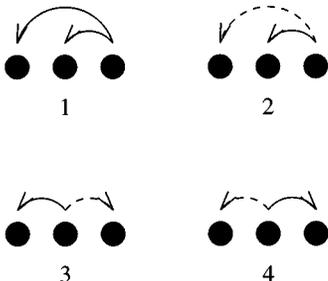
FIG. 3. Helicity exchange in the one-triad system for the four models. Dashed (solid) arrows point towards the mode that receives less (more) helicity.
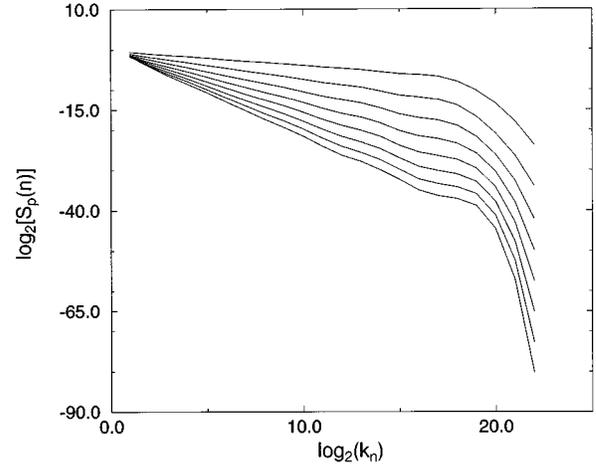
FIG. 4. Logarithm $\log_2[S_p(n)]$ of the structures functions of model 3 vs $\log_2(k_n)$. The parameters values are $\alpha=1$ and $\lambda=2$.

$$S_p(n)=\langle|\tilde{u}_n|^p\rangle, \tag{25}$$

where $\tilde{u}_n=\sqrt{|u_n^+|^2+|u_n^-|^2}$. In Fig. 4 we show $\log_2[S_p(n)]$ as a function of $\log_2(k_n)$ for $p=1,\ldots,8$. There is a well defined inertial range where the structure functions follow a power law

$$S_p(n)\sim k_n^{-\zeta(p)}. \tag{26}$$

Let us note that in this model, at variance with the GOY model, there are no period-three oscillations superposed on the power-law scaling. In this case a linear least-square fit allows one to compute the scaling exponents $\zeta(p)$ with an uncertainty smaller than in the GOY model.

Nevertheless, in order to have a better estimate of the $\zeta(p)$'s one can study the moments of a particular third-order quantity: the mean energy flux through the nth shell

$$\Pi(n)=2k_n\mathrm{Im}\left[\langle u_{n+2}^{s_1}u_{n+1}^{s_2}u_n^+\rangle+b_3\langle u_{n+1}^{s_3}u_n^+u_{n-1}^{s_4}\rangle\right.$$
$$+\frac{1}{\lambda}\langle u_{n+1}^{s_1}u_n^{s_2}u_{n-1}^+\rangle+\langle u_{n+2}^{-s_1}u_{n+1}^{-s_2}u_n^-\rangle$$
$$\left.+b_3\langle u_{n+1}^{-s_3}u_n^-u_{n-1}^{-s_4}\rangle+\frac{1}{\lambda}\langle u_{n+1}^{-s_1}u_n^{-s_2}u_{n-1}^-\rangle\right], \tag{27}$$

where s_1, s_2, s_3, and s_4 for model 3 are taken from Table I. As pointed out by Pisarenko et al. [16], one can write for this quantity the equivalent of Kolmogorov's four-fifths law, expressing the balance between energy input and energy dissipation in the system.

Considering the energy variation over the first n shells
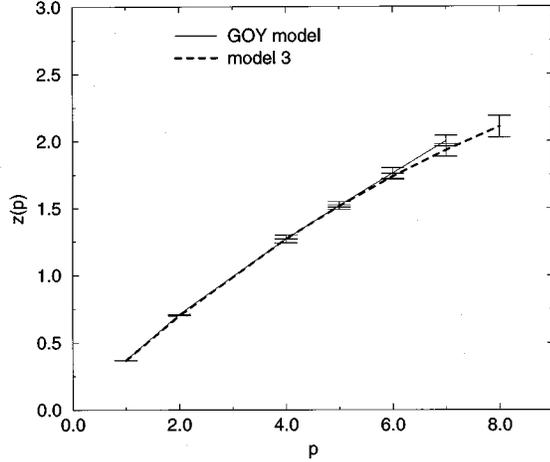
FIG. 5. $\zeta(p)$'s of the GOY model (from [17]) and model 3. The parameters values are $\alpha=1$ and $\lambda=2$. Error bars for data concerning model 3 take into account both statistical and power-law fit errors.

$$\frac{d}{dt}\left[\sum_{m=1}^{n}(\langle|u_m^+|^2\rangle+\langle|u_m^-|^2\rangle)\right]$$

$$=-2\nu\sum_{m=1}^{n}k_m^2(\langle|u_m^+|^2\rangle+\langle|u_m^-|^2\rangle)+\Pi(n)$$

$$+2\,\mathrm{Re}[\langle f^+u_{n_0}^{+\,*}\rangle+\langle f^-u_{n_0}^{-\,*}\rangle] \tag{28}$$

and assuming a statistical steady state, in the limit of vanishing viscosity we are left with an inertial range in which $\Pi(n)$ is constant:

$$\Pi(n)\sim\mathrm{const.} \tag{29}$$

In analyzing the scaling properties of all our results we have always used extended self-similarity (ESS). ESS consists of plotting one structure function versus another $[S_3(n)$, for example]. ESS ends up improving the precision with which scaling exponents can be measured in true turbulent flows [3,4] and in shell models [15].

We have applied ESS analysis to two kinds of fit: $\log_2[S_p(n)]$ vs $\log_2[S_3(n)]$ and $\log_2[\Sigma_p(n)]$ vs $\log_2[\Sigma_3(n)]$, where

$$\Sigma_p(n)=\langle|\Pi(n)/k_n|^{p/3}\rangle. \tag{30}$$

In all our simulations we have found the two sets of exponents coinciding within the numerical and statistical errors.

Figure 5 shows the $\zeta(p)$'s of model 3, compared with those of the GOY model with the same parameters $\alpha=1$ and $\lambda=2$ (corresponding to the classical choice, which conserves the analog of the 3D helicity). The scaling is nearly the same. Indeed, we argued in Sec. IV that both models have a forward energy flux; what turned out to be different was the exchange of helicity among shells, together with a different sensitivity on the parameter α connected to this second invariant. What occurs is a strong similarity for $\alpha=1$; nevertheless, we expect a different behavior when this parameter is allowed to vary.
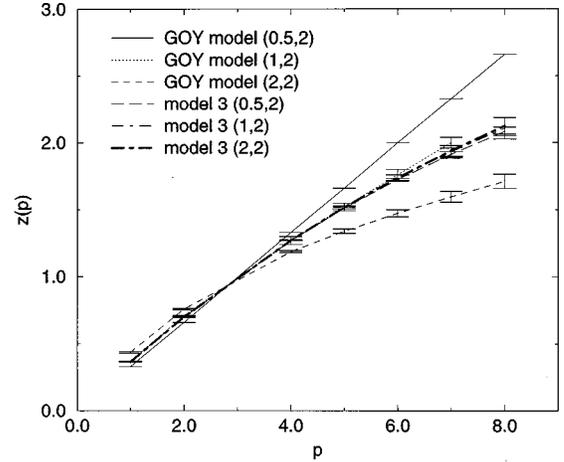
FIG. 6. $\zeta(p)$'s of the GOY model and model 3 for different parameters sets (α,λ). λ is always kept equal to 2. The $\zeta(p)$'s $(p=1,\dots,7)$ for the GOY case $(1,2)$ are taken from [17]. Notice that for model 3 all data sets collapse on the same curve for different α values. Error bars for data concerning model 3 take into account both statistical and power-law fit errors.

A. The α dependence

For the α dependence of the models we have explored two other different values: $\alpha=0.5$ and 2 (keeping fix $\lambda=2$). It is well known [15,17,18] that the GOY model shows a strong dependence of its statistical properties on the α value. For example, if $\alpha<\frac{2}{3}$, the dynamics is attracted toward a fixed point with Kolmogorov scaling, $\zeta(p)=p/3$. For $\alpha>1$ intermittency become more important than what is usually measured in turbulent flows [17] On the other hand, the statistical properties of model 3 turn out to be robust under changes of the α parameter.

In Fig. 6 we show the $\zeta_\alpha(p)$ exponents for the GOY model and model 3 at $\alpha=0.5,1,2$. Clearly, there is an evident dependence of the $\zeta(p)$'s on α for the GOY case, while for model 3 the different exponents coincide within numerical errors. This behavior is in perfect agreement with the phenomenological speculations argued in Sec. IV from the study of the single-triad system. The robustness of model 3, with respect to variation in α, gives this model an important role among the possible shell models of turbulence.

B. The λ dependence

Concerning the dependence on the scale parameter λ, we have performed an exploratory study by fixing $\alpha=1$ and taking $\lambda=1.5$ and 2.5 in model 3. For the case with $\lambda=2.5$ the $\zeta(p)$ exponents are still stuck to the previous values at $\lambda=2$. On the other hand, for the case $\lambda=1.5$ we found a weak discrepancy, comparable with the one found in [17] for the GOY model. The issue of what happens in the limit $\lambda\to1$ (the so-called continuum limit) is one of the most intriguing problems that must be analyzed in both cases: the GOY model and model 3 (see Sec. VI).

In Fig. 7 we show three sets of exponents obtained for different choices of λ for both model 3 and the GOY model. The origin and significance of the weak spreading in the values of $\zeta(p)$ is far from being understood. By changing λ, one changes the ratio between adjacent shells and there-
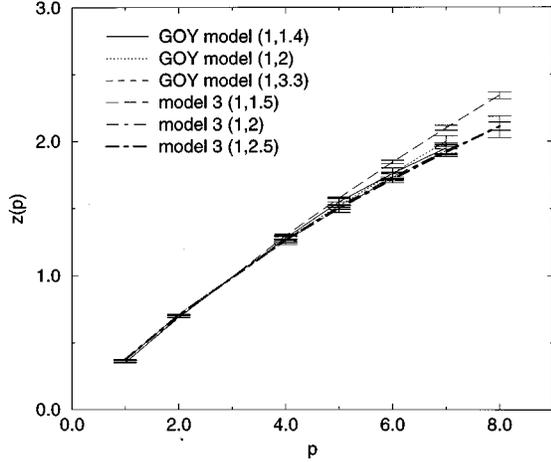
FIG. 7. $\zeta(p)$'s of the GOY model and model 3 for different parameters sets (α, λ). α is always kept equal to 1. The $\zeta(p)$'s ($p = 1, \ldots 7$) for the three GOY cases are taken from [17]. Notice that for one value of λ ($\lambda = 1.5$) our numerically evaluated $\zeta(p)$'s are slightly different from those found in the GOY model and in model 3 for other λ values. We are not able to conclude whether or not this discrepancy is important. Error bars take into account both statistical and power-law fit errors.

fore how viscous and inertial ranges match together. This nontrivial matching might interfere also with the determination of the scaling exponents [26].

The λ dependence in all these shell models is, however, a very important open question due to the obvious interest in having a PDE describing the continuum limit ($\lambda \to 1$) of the energy transfer. In the following section we derive the equation for the continuum limit of all four models and we present some proposal for further investigations.

VI. THE CONTINUUM LIMIT

As anticipated in the preceding section, one of the most interesting and still unexplored aspects of GOY-like shell models is their dynamics in the continuum limit [27]. For the continuum limit we intend the limit when the separation between shells goes to one, i.e., $\lambda \to 1$,

$$k_{n+1} = \lambda k_n \sim (1 + \delta) k_n, \tag{31}$$

where we have defined $\lambda = \exp(\delta) \sim 1 + \delta + O(\delta^2)$. In the limit (31) we can expand the u_n set as

$$u(k_{n+m}) = u(k_n) + \delta m k_n \partial_k u(k_n) + O(\delta^2). \tag{32}$$

Taking into account the equivalent expansions for the a, b, c coefficients (see Table II) and after some simple algebra one realizes that all three models (models 1, 2, and 3) lead to the same expression in the continuum, namely,

$$\partial_t u^+(k) = ik[4ku^- \partial_k u^+ + 2ku^+ \partial_k u^- + (2 + \alpha)u^+ u^-$$
$$- \alpha u^- u^-]^* - \nu k^2 u^+ + f(k). \tag{33}$$

The corresponding equation for the $u^- s$ is obtainable from (33) by changing all helicity indices.

This PDE warrants a deeper study for many reasons. First, let us note that the continuum limit is highly nonreversible, i.e., trying to return to a logarithmically equispaced shell structure, one does not recover the original equations (18). Second, the continuum model shows an unexpected universality: It is the limit of three models that have very different behaviors at $\lambda > 1$. Third, even in the continuum there are two conserved quantities (in the unforced and inviscid limit) corresponding to the continuum analogous of energy and generalized helicity:

$$E = \int \frac{dk}{k}(|u^+|^2 + |u^-|^2), \quad H_\alpha = \int \frac{dk}{k} k^\alpha(|u^+|^2 - |u^-|^2), \tag{34}$$

where the, apparently unusual, dk/k integration step comes from the original logarithmically equispaced shell structure. Let us remark that the most interesting difference between the continuum expression (33) and the analog for the original GOY model is that now in (33) helicity conservation is also well defined. This was not the case for the continuum GOY model. The apparent paradox (model 1 is formed by two uncorrelated GOY models when $\lambda > 1$) is easily solved by noticing that in the continuum limit shells collapse in such a way that the original ordering is destroyed. This limiting procedure introduces a coupling between the two submodels.

This drastic difference with the GOY continuum case suggests the possibility that this alternative set of PDEs has a much richer dynamics than the corresponding GOY PDEs. In that case it is indeed quite easy to realize that PDEs are integrable along the characteristics [28] (at least for the case of real variables). The solutions have a burstlike shape with Kolmogorov scaling, reaching infinite k at finite time (for zero viscosity). Whether or not Eqs. (33) are more interesting is still an open question.

As for the continuum limit of model 4 we need to go the second order in the δ expansion to obtain

$$\partial_t u^+(k) = ik[16k^2(\partial_k u^+)^2 + 2k^2 u^+ \partial_k^2 u^+$$
$$+ 12(\alpha + 2)ku^+ \partial_k u^+ + (\alpha + 2)^2(u^+)^2]^*$$
$$- \nu k^2 u^+ + f(k). \tag{35}$$

In this case the continuum limit is much more similar to what should be the continuum limit of a shell model describing 2D turbulence. The only two conserved quantities are both positive definite and coincide with energy and with a generalized enstrophy Ω_α. A much more detailed investigation of both models is postponed to a future study.

VII. CONCLUSION

In this paper a detailed investigation of a different class of helical shell models derived from the helical decomposition of interactions between Fourier modes in Navier-Stokes equations has been investigated. Four distinct types of shell models are identified, each conserving two inviscid quadratic quantities analogous to energy and helicity in the three-dimensional Navier-Stokes equations. Two of these four models (models 1 and 4) coincide with the 3D and 2D versions of one of the most studied shell models, the GOY model, that is, these versions of the GOY model have statis-

tical properties that match three- and two-dimensional turbulence, respectively.

The other two models (models 2 and 3) show different and peculiar properties. Most of the numerical results presented in this paper concern model 3, which has been found to be more stable under changes of its free parameters than the original GOY model. The different feature of model 2 identified in preliminary simulations is the presence of a significant backward energy transfer, which leads to possibly strong deviations from the Kolmogorov scaling. A detailed study of model 2 is planned for the future [29]. Why such different and severe truncations of Navier-Stokes equations yield such a variety of dynamical behavior is certainly the most stimulating result to develop from this study. Also, the crucial role played by inviscid invariants, especially in the presence of two simultaneous transferred quantities, is confirmed.

The main result presented here is the strong universality shown by model 3 at varying the physical dimension of the second invariant. This can be partially understood by invoking the tendency of each single shell to transfer helicity backward and forward simultaneously, leading to a net vanishing of helicity flux. There is nothing from these studies of uncoupled chains, that is, models 1–4 are not coupled, to suggest any preference between models 1 and 3. Without the effects of intermittency inherent in shell models, a two-point closure based on the helicity decomposition discussed here [30] suggests a preference for model 1, which is the GOY model. A better understanding of why model 3, from all the possible types of intermittent statistics, has exactly the same statistics as found in Navier-Stokes equations could help resolve some of these issues.

The longer term objective of the program established here is to provide a basis for direct numerical simulations of turbulence and analyses of those simulations. The premise is that if shell models with just a few paths are reproducing some aspect of the intermittent dynamics of turbulence, some signature of these paths should exist in full simulations. Our hope is that the rich behavior of the four models studied here could help identify what this signature might be in the Navier-Stokes equations. For example, could one recognize when significant back transfer of energy, such as in models 2 and 4, might occur? Could one recognize instances where different signs of the sensibility of helicity can be identified, such as in models 1 and 3?

In addition, there are some serious questions coming from statistical studies of turbulence that must also be addressed in this process. Note that extrapolating strongly dissipative effects such as intermittency using the usual arguments of absolute equilibrium behavior [31,25] seems to fail for this class of shell model. Indeed, starting from the analysis of absolute equilibrium, one should conclude that by changing α, and therefore the dimension of the second invariant, the inertial properties in the dissipative case should change. This is definitely true in the GOY model, but definitely false in model 3.

Some concern has been expressed that shell models with only one or two paths for the cascade to follow are too strongly constrained to properly represent the turbulent cascade. For example, by increasing the number of modes and interactions per shell, nonintermittent behavior is obtained [32,33]. This is generally understood as due to the existence of multiple paths for the cascade to follow. Since the full Navier-Stokes equations could be viewed as a shell model with a very large number of modes per shell, why do the statistics of turbulence resemble the single-path GOY model (or model 3) instead? What this might suggest is that there is some type of prescribed path that the cascade in turbulence follows that would be analogous to the two models. What guides this path in Fourier space might be physical space structures such as vortex tubes [5,34] or singularities [35,36]. Further, by comparison with the other models in the class studied here one might understand that the GOY model and model 3 represent simply the preferred path.

[1] A. N. Kolmogorov, Dokl. Akad. Nauk SSSR **30**, 9 (1941).

[2] C. Meneveau and K. R. Sreenivasan, J. Fluid Mech. **224**, 429 (1991).

[3] R. Benzi, S. Ciliberto, R. Tripiccione, C. Baudet, C. Massaioli, and S. Succi, Phys. Rev. E **48**, R29 (1993).

[4] R. Benzi, S. Ciliberto, C. Baudet, and G. R. Chavarria, Physica D **80**, 385 (1994).

[5] R. M. Kerr, J. Fluid Mech. **153**, 31 (1985).

[6] L.-P. Wang, S. Chen, J. G. Brasseur, and J. C. Wyngaard, J. Fluid Mech. **309**, 113 (1994).

[7] R. M. Kerr, J. Fluid Mech. **211**, 309 (1990).

[8] R. Benzi, G. Paladin, G. Parisi, and A. Vulpiani, J. Phys. A **17**, 3521 (1984).

[9] C. Meneveau and K. R. Sreenivasan, Phys. Rev. Lett. **59**, 1424 (1987).

[10] Z. S. She and E. Leveque, Phys. Rev. Lett. **72**, 336 (1994).

[11] B. Dubrulle, Phys. Rev. Lett. **73**, 959 (1994).

[12] E. B. Gledzer, Dokl. Akad. Nauk SSSR **208**, 1046 (1973) [Sov. Phys. Dokl. **18**, 216 (1973)].

[13] M. Yamada and K. Ohkitani, Prog. Theor. Phys. **81**, 329 (1989); J. Phys. Soc. Jpn. **56**, 4210 (1987); Phys. Rev. Lett. **60**, 983 (1988); Prog. Theor. Phys. **79**, 1265 (1988).

[14] M. H. Jensen, G. Paladin, and A. Vulpiani, Phys. Rev. A **43**, 798 (1991).

[15] L. Biferale, A. Lambert, R. Lima, and G. Paladin, Physica D **80**, 105 (1995).

[16] D. Pisarenko, L. Biferale, D. Courvoisier, U. Frisch, and M. Vergassola, Phys. Fluids A **65**, 2533 (1993).

[17] L. Kadanoff, D. Lohse, J. Wang, and R. Benzi, Phys. Fluids **7**, 617 (1995).

[18] L. Biferale and R. Kerr, Phys. Rev. E **52**, 6113 (1995).

[19] J. C. André and M. Lesieur, J. Fluid Mech. **81**, 187 (1977).

[20] W. Polifke and L. Shtilman, Phys. Fluids A **1**, 2025 (1989).

[21] R. M. Kerr and E. D. Siggia, J. Stat. Phys. **19**, 543 (1978).

[22] F. Waleffe, Phys. Fluids A **4**, 350 (1992).

[23] P. Frick, B. Dubrulle, and A. Babiano, Phys. Rev. E **51**, 5582 (1995).

[24] E. Aurell, G. Boffetta, A. Crisanti, P. Frick, G. Paladin, and A. Vulpiani, Phys. Rev. E **50**, 4705 (1994).

[25] P. D. Ditlevsen and I. A. Mogensen (unpublished).

[26] N. Schoerghofer, L. Kadanoff, and D. Lohse, Physica D **86**, 1 (1995).

[27] G. Parisi (unpublished).

[28] D. Lohse (private communication).

[29] R. Benzi, L. Biferale, and E. Trovatore (unpublished).

[30] F. Waleffe, Phys. Fluids A **5**, 677 (1993).

[31] R. Kraichnan, J. Fluid Mech. **59**, 745 (1973).

[32] S. Grossman and D. Lohse, Phys. Rev. E **50**, 2784 (1994).

[33] O. Gat, I. Procaccia, and R. Zeitak, Phys. Rev. E **51**, 1148 (1995).

[34] Z.-S. She, E. Jackson, and S. O. Orszag, Proc. R. Soc. London Ser. A **434**, 101 (1991).

[35] R. M. Kerr, Phys. Fluids A **5**, 1725 (1993).

[36] G. Parisi and U. Frisch, in *Turbulence and Predictability in Geophysical Fluid Dynamics*, Proceedings of the International School of Physics "Enrico Fermi," Course LVII, Varenna, 1983, edited by M. Ghil, R. Benzi, and G. Parisi (North-Holland, Amsterdam, 1985), p. 84.